Reply to Interactive comment on "Thin-ice dynamics and ice production in the Storfjorden polynya for winter-seasons 2002/2003–2013/2014 using MODIS thermal infrared imagery" by A. Preußer et al.

Received from anonymous referee #1

This paper describes the spatial and temporal characteristics of the Storfjorden polynya over a time period of more than 10 years using thermal infrared satellite imagery. The paper is well written and easy to follow. The method to calculate ice thickness from MODIS is well-known, and already published in other papers. However, the statistical analysis of polynya using MODIS data over such a long time period is valuable and the method could be extended to other regions with frequent polynya openings and respective ice production which are important for the ocean circulation. Therefore, the paper is worth to be published with minor revisions.

We would like to thank the first referee for her/his valuable comments and suggestions that will definitely help to improve the original manuscript, most importantly the discussion and the specification of error-margins. We carefully went over the mentioned parts of the manuscript and we will answer specific and general comments in the following.

Specific comments:

P. 5764, L. 11-13. *It is not clear to me, if "an increasing frequency" is meant for one freeze-up period or a trend in the 12 years period here.*

The number of larger polynya events in Nov.-Dec. increases over the regarded 12-yr period, not one single freeze-up period.

We slightly changed the formulation in the Abstract to make that more clear.

P. 5765, L. 11. *Please add references after "model approaches".*

We added Ebner et al. (2011), Krumpen et al. (2011) and Bauer et al. (2013) as reference.

P. 5765, L. 15-21. *There are also other regions with frequent polynya openings and active ice production in the Arctic (e.g. Laptev Sea). Why is the Storfjorden region so important that you choose this region for the statistical analysis?*

The selection of our study area followed several distinct requirements: 1) A comparatively small areal extent to profit from enhanced resolution imagery. 2) A region that is well studied to compare our estimates. 3) More or less stable formation-mechanism with limited error-sources (e.g. oceanic heat input). 4) Significant importance considering total IP and deep water formation. 5) Part of the study area during the aircraft-based campaign LEAST (March 2014)

We will add some statements to the revised manuscript.

P. 5765, L. 26-29. *How do you intend to distinguish the sea ice transported into the Storfjorden area from thermodynamically induced ice growth? Could this be a factor of uncertainty in your estimates?*

Sea ice that is advected from the south into Storfjorden may play a role in the total ice thickness distribution. But, as our ice production estimates are based on the "as is" daily mean thin-ice thickness distribution below 20 cm ice thickness, these processes are included in our estimates as long as the total ice thickness in a certain grid cell does not exceed 20 cm.

P. 5766, L. 24. *"IST swath"→ "Swath-based IST"*

We fixed that, thank you for your suggestion.

P. 5767, L. 5. *Please emphasize here that only nighttime scenes are used in this study.*

We changed it to "(…) resulting in 27 individual swaths per day on average for later composite generation. These composites solely consist of nighttime scenes to exclude the influence of incident shortwave radiation (Yu and Lindsay (2003), Adams et al. (2013); compare Ch. 2.3 and 2.3.1). (…)".

P. 5767, L. 11. *Please add references after "previous studies".*

Added Skogseth et al. (2004, 2005) and Jardon et al. (2014) as reference.

P. 5769, L. 29. *The uncertainty of the retrieved TIT caused by neglecting a snow layer should be discussed here.*
First, we think that this assumption is valid for very thin ice (compare Adams et al., 2013: "*we neglect snow on the thin ice, which is in accordance with in situ observations [in the Laptev Sea] during the TRANSDRIFT XV expedition*"). Similar observations could be made in March 2014 during the aircraft-based campaign LEAST in Storfjorden. Of course these are only airborne observations for a few cases, so we can't exclude any possible snow layer in general. Mäkynen et al. 2013 applied a snow layer thickness in the TIT-retrieval, based on a statistical relationship to the ice thickness. Although this approach seems to work reasonably well, we decided not to use it as (to our best knowledge) there are no reference / validation measurements for snow on thin ice (below 0.2 m) available.
As we are currently not trying to develop a new procedure of handling a possible snow cover, we decided to stick to the assumption formulated by Drucker et al. (2003) and Adams et al. (2013).

P. 5772, L. 16. *"SD are highest'→ "SD is highest"*

We fixed that, thank you for your suggestion.

P. 5772, L. 1. *Please define the "relative TIT-distributions".*

We changed the mentioned part into: "The bars in Fig.3 show the mean relative contribution of each ice-thickness class from the total number of pixels with a TIT-value ≤ 0.2 m between the winter-seasons 2002/2003 to 2013/2014."

Section 4 Discussion

Question 1: *What could be the potential reason of positive trend in IP in the Storfjorden region during the last 12 winter-seasons? Fig. 8 shows an extremely high IP during the winter season of 2012/2013. Do you have any explanation?*

We find that the significant positive trend in overall (Nov.-Mar.) IP_{CC} originates primarily from a significant positive trend (CC: 1.29km³/yr, p = 9.05*10^-4) at the beginning of winter (Nov.-Dec.), while the period from Jan.-Mar. shows no significant trend (but still being positive; CC: 0.73km³/yr, p = 0.052). This could be an effect of an observable shift towards more thin-ice in Nov.-Dec., which is most probably connected to a later appearing fall freeze-up (as already mentioned in the manuscript) and therefore a lot open water / very thin ice in the southern part of the applied polynya-mask. A similar explanation can be given for the high IP in 2012/2013, where the Storfjorden area features high frequencies of TIT ≤ 0.2 m not only in Nov.-Dec., but also in Jan.-Mar. This could be related to an anomalous northerly position of the ice-edge in Storfjorden.

We will add some words about that topic in the results and discussion. An alternative version of Fig.8 which highlights seasonal differences in IP is shown below.
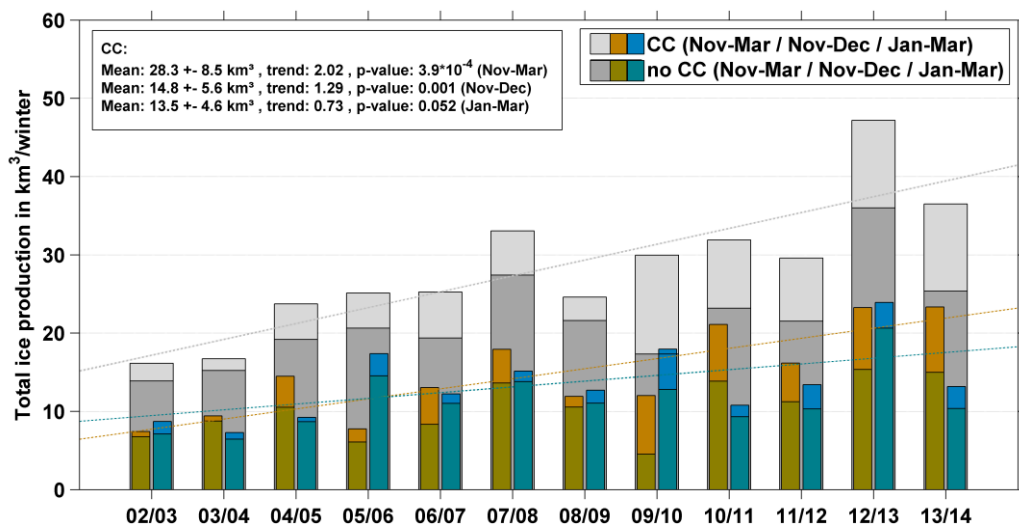

Figure 1 Annual wintertime accumulated ice production in the Storfjorden polynya, given in km³/winter. Estimations are based on daily heat flux calculations using the daily derived TIT- composites. Special emphasis is given to the effect of an applied coverage correction (CC). Dotted lines show linear trend estimations for IP_CC. Colored bars are additionally given for a seasonal comparison between November-December (yellowish) and January-March (blueish).

Question 2: *Does the coarse resolution of sea ice concentration derived from passive microwave sensors lead to the overestimation of IP in this region? If yes, what is the reason?* It leads for sure to a higher uncertainty, while the sign of the bias cannot be determined here. It will depend on the distribution of thin ice within the sensor's footprint and potential land spillover effects.

Question 3: *As you mentioned, MODIS data has a strong limitation due to the cloud coverage. Please discuss in more detail how large is the uncertainty of IP estimate due to the cloud coverage.*

Thank you for your remark. This topic was also mentioned by the other two referees, so we decided to perform and include an error analysis as proposed by anonymous referee No.3.

To test the performance of our coverage-correction scheme, which aims at compensating cloud-induced data gaps, we selected a total of six case studies from January 2009, which feature more or less clear-sky conditions (≥ 99%; IST-coverage → percentage of pixels within

the polynya mask that feature at least one valid IST-value from all MOD/MYD29 swaths covering the Storfjorden region at a given day). The coverage-correction has been iteratively (n = 1000) applied for each case study after randomly removing 45% of the pixels within the polynya mask. The resulting deviation (in %) from the "true" polynya area (POLA) from all case studies combined is shown in the Figure below. These $POLA_{CC}$-deviations almost perfectly follow a typical normal (Gaussian) distribution, with a mean value of 0.67% (in a hypothetical case of 100% IST-coverage we expect it to be ± 0) and a standard error of ~ 5-6 % of the daily POLA. This may help to quantify the error of our method.

Alternatively, we think that interpolating between bounding days with better IST-coverage (> 50%) is so far the best solution of handling large cloud-gaps in the daily composites. For future studies, we are working on a more advanced solution which incorporates a spatial feature reconstruction algorithm.

As the correction / upscaling of IP-values uses the same scaling-factor F, the retrieved error-margins can also be regarded as the uncertainty of our IP_{CC} estimates.

We will add this information in the revised manuscript in Ch.2.3.3 and plan to include a short appendix.

Question 4: *Only from this paper, I could not conclude that the Storfjorden polynya has special contribution to the overall ice production in the Arctic. Could you give an approximate estimation of the contribution of IP from Storfjorden to the Arctic-wide IP?*

According to Iwamoto et al. (2014), the Storfjorden polynya contributes with 4 % to the average total ice volume produced in Arctic polynyas between 2002/2003 and 2010/2011 (September-May), which appears to be a minor contribution. Despite that, the Storfjorden polynya is highly relevant due to its importance on deep water formation and the connection of the water masses in Storfjorden to the larger-scale ocean dynamics in the Barents and Greenland Seas. Estimations by Skogseth et al. (2004) show that the Storfjorden polynya supplies between 5-20% of all the newly formed dense water (BSW) which enters the Arctic Ocean, although its spatial extent is comparatively small.

We will add some additional words dealing with the pan-arctic context / relevance in the discussion. In addition, we would like to mention at this point that we are currently preparing a follow-up study dealing with pan-arctic TIT-retrievals and IP-estimates. This will enable us to do direct comparisons between the most important Arctic polynya-regions.

Reply to Interactive comment on "Thin-ice dynamics and ice production in the Storfjorden polynya for winter-seasons 2002/2003–2013/2014 using MODIS thermal infrared imagery" by A. Preußer et al.

Received from anonymous referee #2

The MS presets an application of the previously developed algorithm (Adams et al., 2013) of deriving thin sea ice thickness (<20cm) from MODIS SIT products and other datasets, for the Storfjorden polynya for the winter season of 2002-2014 period. The tech is clear and results are compared with others, and showing clear advantage and reliability of the results. I can recommend the paper to be published only after authors address those comments below and maybe more in the revision stage.

We would like to thank the second referee for her/his valuable comments and suggestions that will definitely help to improve the original manuscript (MS). We carefully went over the specified parts in the MS and we will answer her / his comments in the following.

Specific comments:

(1) *In page 5767, line 1, you mentioned the MODIS SIT is for daytime only, no nighttime validation has been done. But you used this data for the winter season which is nighttime only (no daytime), right? So how you can use those data? Am I wrong? I realized this same data was used in the Adams et al. (2013) paper.*

Thank you for this valuable comment, which motivated us to review the cited studies by Hall et al. (2004) and Riggs et al. (2006) more carefully.

First of all, it is correct that we only used nighttime scenes in our investigation to exclude ambiguities originating from the inclusion of shortwave radiation. Regarding the nighttime validation of MODIS IST, we discovered that apparently there is a small error in the study of Riggs et al. (2006). Hall et al. (2004) present an accuracy assessment using both Arctic (buoys and meteorological data from tide stations) and Antarctic (South Pole station) validation data sets. Thereby, an IST-accuracy (RMSE) of 1-3 K is given, which depends on location, sample size, a certain temperature bias and different criteria for cloud screening. In addition, it is clearly stated that also nighttime cases are included (especially for the Antarctic IST-validation: 255 cases which are primarily nighttime cases (April–December 2001)). Therefore, we have no reason to assume a worse IST-accuracy / sensor-calibration for nighttime MODIS swaths than during daytime, besides an increased tendency to be affected by undetected cloud signals / decreased performance of the MOD35 cloud mask (lack of visible channels for the cloud mask). The used coefficients in the split-window approach to calculate IST from satellite measured brightness temperatures are not dependent on day-/nighttime conditions.

Consequently, we will leave out the sentence about a missing nighttime validation and correct the accuracy range to 1-3 K, as it was done in several comparable studies using nighttime MODIS IST data.

(2) *In page 5768 line 20, there is an assumption of $Q_{atm} = Q_{ice}$, I would like authors to address this for possible error and why this assumption stands.*
First of all, this is exactly what the surface energy balance requires. The critical question is, if a bulk approach for heat conduction can be used.
By using an upper threshold of 50 cm for TIT-calculations (Yu and Rothrock, 1996; Drucker et al., 2003), the vertical temperature gradient in the ice can be assumed to be linear according to Stefan's law (Stefan, 1891). Yu and Rothrock (1996) state: "This assumption (i.e. linear temperature profile) is supported both by field observations (Nakawo and Sinha, 1981) and by a theoretical study (Maykut, 1982)."

(3) Page 5771 equations 4,5, you have one assumption, assuming the polynya area has the same proportion under cloud cover and no cloud cover; and your correction was only applied to coverage (make clear what coverage?) over 0.5. I think both of these will cause errors and I hope you can discuss them.

Thank you for your remark. This topic was also mentioned by the other two referees, so we decided to perform and include an error analysis as proposed by anonymous referee No.3.

We selected a total of six case studies from January 2009, which feature more or less clear-sky conditions (≥ 99%; IST-coverage → percentage of pixels within the polynya mask that feature at least one valid IST-value from all MOD/MYD29 swaths covering the Storfjorden region at a given day). The coverage-correction has been iteratively (n = 1000) applied for each case study after randomly removing 45% of the pixels within the polynya mask. The resulting deviation (in %) from the "true" polynya area (POLA) from all case studies combined is shown in the Figure below. These POLA$_{CC}$-deviations almost perfectly follow a typical normal (Gaussian) distribution, with a mean value of 0.67% (in a hypothetical case of 100% IST-coverage we expect it to be ± 0) and a standard error of ~ 5-6 % of the daily POLA. This may help to quantify the error of our method.

Alternatively, we think that interpolating between bounding days with better IST-coverage (> 50%) is so far the best solution of handling large cloud-gaps in the daily composites. For future studies, we are working on a more advanced solution which incorporates a spatial feature reconstruction algorithm.

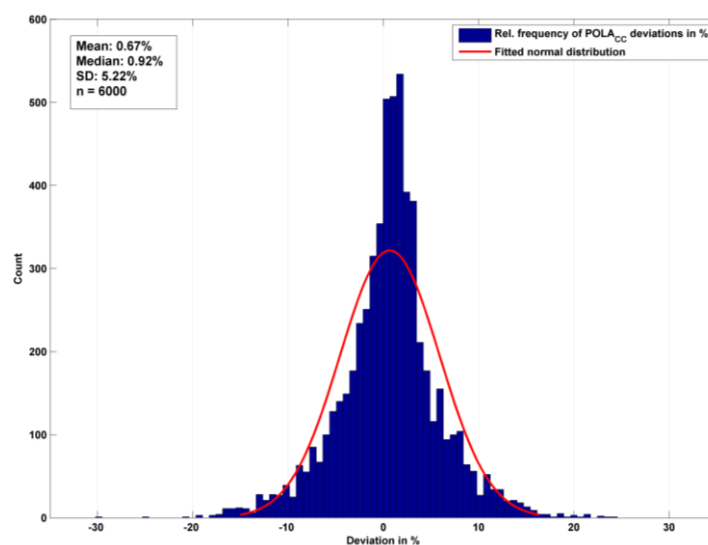We will add this information in the revised manuscript in Ch.2.3.3 and plan to include a short appendix.

*Figure 1 Histogram of POLA$_{CC}$-deviations, based on six near clear-sky case studies from January 2009 (DOY: 002, 020, 024, 025, 026, 030). For each case study, the coverage-correction was repeated several times (n=1000*6), after randomly removing 45% of the pixels within the applied polynya mask. The red curve illustrates a fitted normal distribution.*

(4) Page 5773 line 15, you mentioned years 2004, 2005, 2007 and 2011, but my checking with the figures, I found they should be 2003, 2004, 2005, 2009 and 2011. Please check.
We checked your comment and indeed, 2003 and 2009 are also fitting to that context. We will add these years in the revised manuscript.

(5) Fig 4 and 5, why only up to 50%?
To enhance the contrast between low and high frequencies, the color-bar is limited to range from 0 to 0.5 (0 - 50% of the days in Nov.-Dec. / Jan.-Mar.).

(6) *I guess those areas of 0 TIT frequency in figure 4, 5 are of thicker ice (>0.2m), I hope you can use the AMSR-E ice concentration maps to support you.*

Thank you for your suggestion. We had a look into daily AMSR-E and AMSR2 SIC-maps for the regarded time period. Due to the coarser spatial resolution and potential ambiguities from land spill-over effects in the comparatively narrow/small Storfjorden area, we decided to leave out the PMW-data in the framework of this study, as it might probably introduce new/additional error sources.

To illustrate the differences between the PMW SIC-data and our TIT-retrievals, we present the spatial distributions of TIT up to 0.2 m (a) and up to 0.5 m (b) as well as the ASI SIC (c) for the 12th of January 2009 in Fig.2 (below). Indeed, areas where pixels show values above 0.2 m compare nicely to higher SIC (more compact ice) in the AMSR-E image. Comparing Fig.2 (b) and (c), you might also notice that there seems to be no direct/simple relationship between thicker ice and higher SIC, as retrieved TIT-values are strongly varying in areas with 100% SIC.
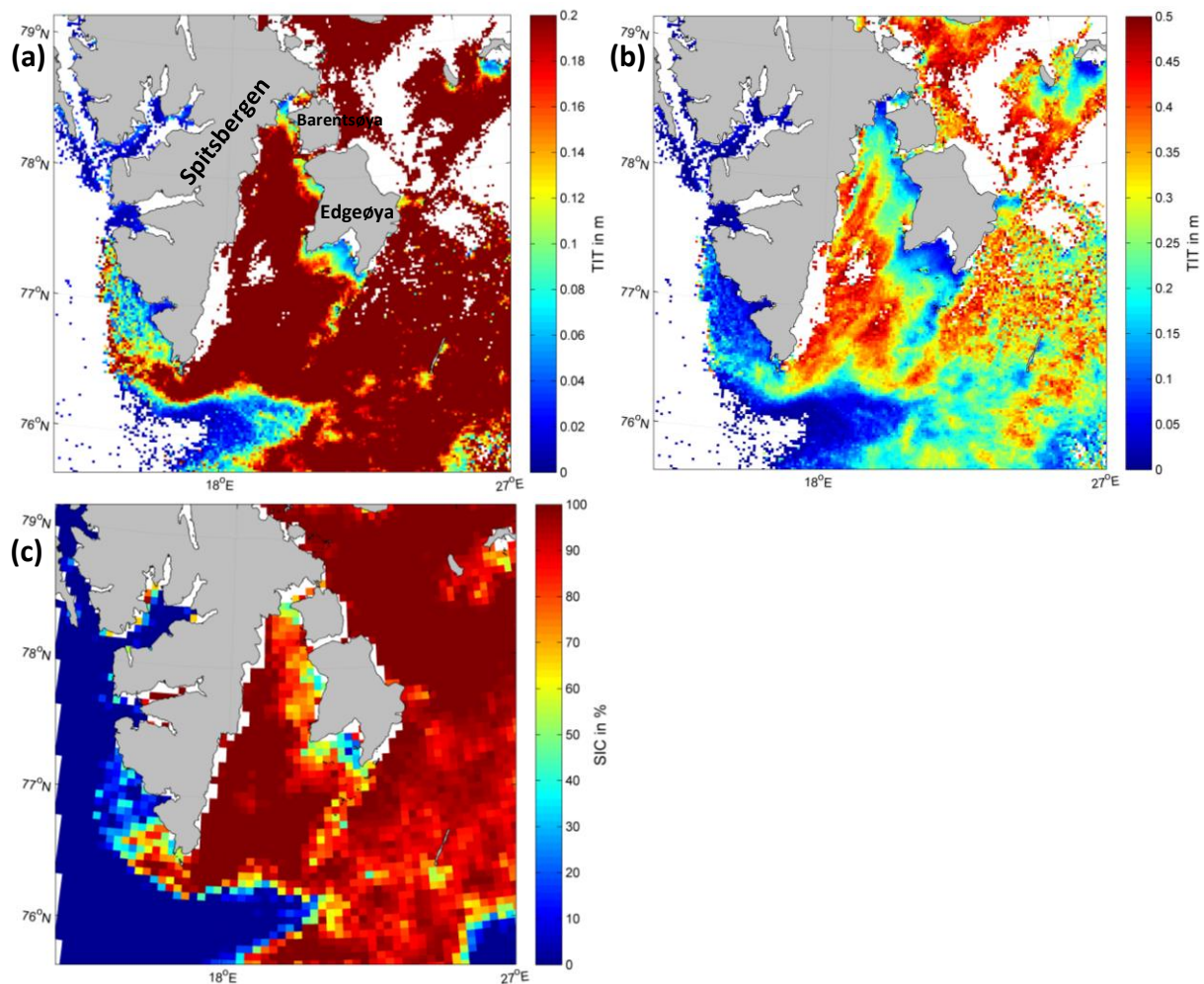

Figure 2 Spatial overview of calculated TIT ≤ 0.2 m (a), ≤ 0.5 m (b) and AMSR-E sea-ice concentrations (ASI v5; University of Bremen; (c)) on the 12th of January, 2009.

(7) *I hope to see more discussion and interpretation on the reasons or mechanisms for such pattern/trend you see from the 12 years of data.*

We find that the significant positive trend in overall (Nov.-Mar.) IP_{CC} originates primarily from a significant positive trend (CC: 1.29km³/yr, p = 9.05*10^-4) at the beginning of winter (Nov.-Dec.), while the period from Jan.-Mar. shows no significant trend (but still being positive; CC:

0.73km³/yr, p = 0.052). This could be an effect of an observable shift towards more thin-ice in Nov.-Dec., which is most probably connected to a later appearing fall freeze-up (as already mentioned in the manuscript) and therefore a lot open water / very thin ice in the southern part of the applied polynya-mask. A similar explanation can be given for the high IP in 2012/2013, where the Storfjorden area features high frequencies of TIT ≤ 0.2 m not only in Nov.-Dec., but also in Jan.-Mar. This could be related to an anomalous northerly position of the ice-edge in Storfjorden.

We will add some words about that topic in the results and discussion. An alternative version of Fig.8 which highlights seasonal differences in IP is shown below.
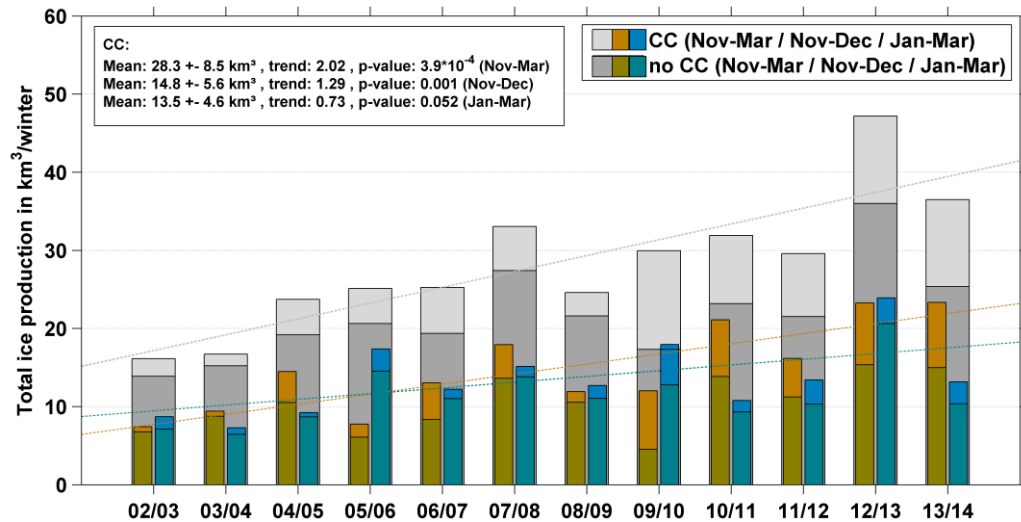

Figure 3 Annual wintertime accumulated ice production in the Storfjorden polynya, given in km³/winter. Estimations are based on daily heat flux calculations using the daily derived TIT- composites. Special emphasis is given to the effect of an applied coverage correction (CC). Dotted lines show linear trend estimations for IP_{CC}. Colored bars are additionally given for a seasonal comparison between November-December (yellowish) and January-March (blueish).

Reply to Interactive comment on "Thin-ice dynamics and ice production in the Storfjorden polynya for winter-seasons 2002/2003–2013/2014 using MODIS thermal infrared imagery" by A. Preußer et al.

Received from anonymous referee #3

General comments:

In the paper the spatial and temporal characteristics of the Storfjorden polynya for the winter seasons of 2002-2014 are described based on thermal infrared satellite imagery. This 12 years data set is the major contribution of the paper. The created data set can be utilized as a reference set to other Arctic polynya statistics and also in the climate simulations. The method to calculate ice thickness from MODIS is well-known generally, and also used by the authors in other papers.

The only significant deficiency in the paper is that the trend and fluctuations observed in the polynya statistics are not set in any manner to a more general context. E.g. connections to the ice conditions in the surrounded seas like the Barents Sea and Fram Strait (or the effect of the Arctic Sea ice retreat generally) are not discussed. Neither any comparisons to other Arctic polynyas, e.g. in the Kara Sea or the Laptev Sea, are made. When these omissions and some other minor points are addressed the paper is worth to be published. I agree with the other referees that the paper is well written and easy to follow.

I have read the reviews by the referees #1 and #2. They raised several important points and questions. I tried to avoid to duplicate the comments already made. Hence I have just a few additional remarks.

We would like to thank the third referee for her/his valuable comments and suggestions for an improved version of the original manuscript. We thoroughly went over the specified parts in the manuscript and we will answer her / his comments in the following.

Specific comments:

P. 5765 (5766?) L5-15*: How does the thermodynamic ice production from the Storfjorden polynya compare to other Arctic polynyas, e.g. polynyas in the Kara and Laptev Seas (see e.g. Kern 2005, 2008 for the Kara Sea and your own publications for the Laptev Sea).*

First, we would like to highlight that a direct comparison to other Arctic polynya systems is challenging, due to a variety of different retrieval methods, strategies and physical parametrizations. Taking this into consideration, the following numbers are worth to be highlighted:
In comparison to other Arctic polynya systems, the Storfjorden polynya is on average quite small (e.g. $POLA_{CC}$ = 4555.7 km² (STO) vs. 21.2 * 10³ km² ± 9.1 * 10³ km² for winters (Jan.–Apr.) 1996/97 to 2000/01 (KARA SEA). Similar differences can be found for the thermodynamic IP derived by either remote sensing techniques (Willmes et al. (2011) → 55.2 km³ (Laptev Sea); Tamura et al. (2011) → 342 ± 71 km³ (Kara Sea); Iwamoto et al. (2014) → 186 ± 34 km³ (North-Water polynya)) or modelling approaches (e.g. Bauer et al. (2013) → 30-73 km³ (Laptev Sea)). Absolute numbers for each region vary dependent on the applied technique and / or regarded spatial margins.
According to Iwamoto et al. (2014), the Storfjorden polynya contributes with 4 % to the average total ice volume produced in Arctic polynyas between 2002/2003 and 2010/2011 (September-May), which appears to be a minor contribution. Despite that, the Storfjorden polynya is highly relevant due to its importance on deep water formation and the connection of the water masses

in Storfjorden to the larger-scale ocean dynamics in the Barents and Greenland Seas. Estimations by Skogseth et al. (2004) show that the Storfjorden polynya supplies between 5-20% of all the newly formed dense water (BSW) which enters the Arctic Ocean, although its spatial extent is comparatively small.

We will add some additional words dealing with the pan-arctic context / relevance in the discussion. In addition, we would like to mention at this point that we are currently preparing a follow-up study dealing with pan-arctic TIT-retrievals and IP-estimates. This will enable us to do direct comparisons between the majority of important Arctic polynya-regions, based on almost the same TIT-retrieval scheme as in the here presented manuscript.

P. 5771. L9-28*. A crucial feature in your approach is the scaling approach. You mentioned it increases the ice volume estimates about 30 %. Hence it is important to have some estimate for the accuracy of the proposed method. This is not difficult to do. Pick a cloud free day, mask 45 % of the polynya area randomly and apply the scaling. When the procedure is repeated several times, you should have understanding how well the approach works. Using three consecutive cloud free days you can get an accuracy estimate for the interpolation procedure. Add the uncertainty estimates to the text and discuss their effect on the results.*

Thank you for this valuable remark and suggestion. As proposed we selected a total of six case studies from January 2009, which feature more or less clear-sky conditions (≥ 99%; IST-coverage → percentage of pixels within the polynya mask that feature at least one valid IST-value from all MOD/MYD29 swaths covering the Storfjorden region at a given day). The coverage-correction has been iteratively (n = 1000) applied for each case study after randomly removing 45% of the pixels within the polynya mask. The resulting deviation (in %) from the "true" polynya area (POLA) from all case studies combined is shown in the Figure below. These $POLA_{CC}$-deviations almost perfectly follow a typical normal (Gaussian) distribution, with a mean value of 0.67% (in a hypothetical case of 100% IST-coverage we expect it to be ± 0) and a standard error of ~ 5-6 % of the daily POLA. This may help to quantify the error of our method.
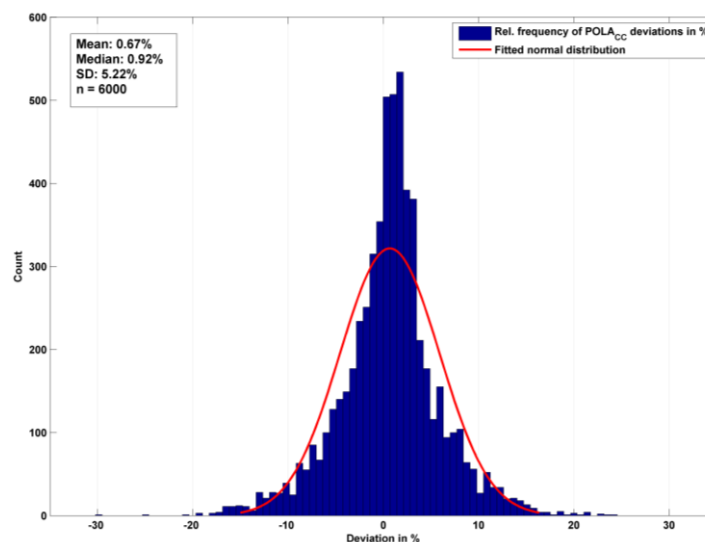

*Figure 1 Histogram of $POLA_{CC}$-deviations, based on six near clear-sky case studies from January 2009 (DOY: 002, 020, 024, 025, 026, 030). For each case study, the coverage-correction was repeated several times (n=1000*6), after randomly removing 45% of the pixels within the applied polynya mask. The red curve illustrates a fitted normal distribution.*

Alternatively, we think that interpolating between bounding days with better IST-coverage (> 50%) is so far the best solution of handling large cloud-gaps in the daily composites. For future studies, we are working on a more advanced solution which incorporates a spatial feature reconstruction algorithm.

We will add this information in the revised manuscript in Ch.2.3.3 and plan to include a short appendix.

P. 5773*. You write in the introduction that time series like this increase our understanding about the Arctic ice conditions. However, you have not linked in any way volume and area estimates of the polynyas to the ice conditions surrounding the Svalbard area, e.g. to ice cover in the Barents Sea and in Fram Strait. Especially interesting these comparisons would be when the IP is very low or very high relative to the mean IP during the covered time period.*
We agree that setting our time series into the context of the sea ice conditions of surrounding areas, other Arctic polynyas, atmospheric conditions (e.g. NAO, AO) would be very interesting. But this is also a little bit beyond the scope of our paper, which should be seen in comparison to related studies in the Storfjorden area.

P. 5774 L. 7-14*. You should analyze the results in Table 2 in more detail. After all those results are one of the main contributions of your paper. When I looked at Table 2 the following points drew my attention: The increase per decade is 7.7-9.5 km3 for the IP estimates (no CC) and 16.1-17.7 km3 per decade for the IP volume estimates with CC. There occur large increases in the IP from winter 2003/2004 to 2004/2005 and again from 2011/2012 to 2012/2013. During the years from 2004 to 2011 the variation in the IP production (with or without CC) is relatively small.*
Thank you for these welcome additions. We will add some more words about that topic at the appropriate parts of the manuscript.
We find that the significant positive trend in overall (Nov.-Mar.) IP$_{CC}$ originates primarily from a significant positive trend (CC: 1.29km³/yr, p = 9.05*10^-4) at the beginning of winter (Nov.-Dec.), while the period from Jan.-Mar. shows no significant trend (but still being positive; CC: 0.73km³/yr, p = 0.052). This could be an effect of an observable shift towards more thin-ice in Nov.-Dec., which is most probably connected to a later appearing fall freeze-up (as already mentioned in the manuscript) and therefore a lot open water / very thin ice in the southern part of the applied polynya-mask. A similar explanation can be given for the high IP in 2012/2013, where the Storfjorden area features high frequencies of TIT ≤ 0.2 m not only in Nov.-Dec., but also in Jan.-Mar. This could be related to an anomalous northerly position of the ice-edge in Storfjorden.

An alternative version of Fig.8 which highlights seasonal differences in IP is shown below.
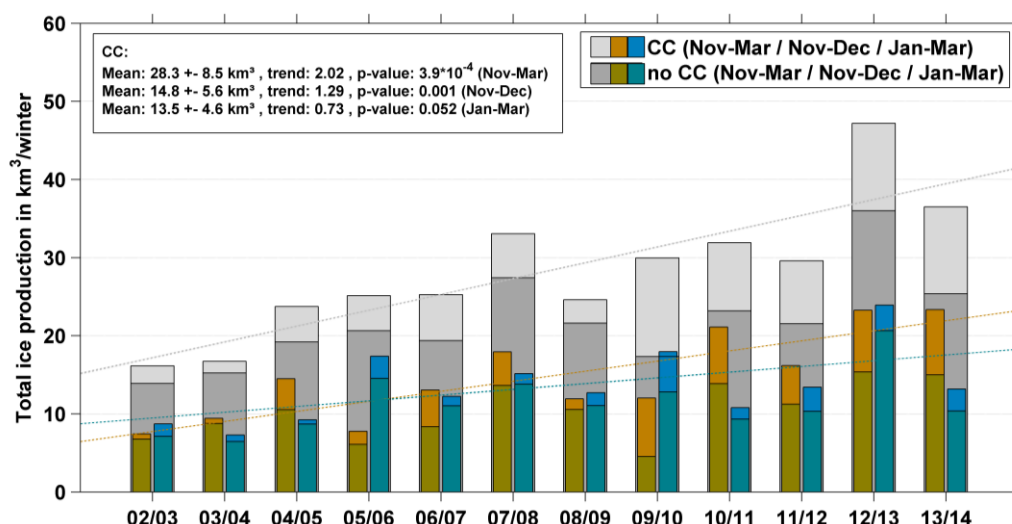

Figure 2 Annual wintertime accumulated ice production in the Storfjorden polynya, given in km³/winter. Estimations are based on daily heat flux calculations using the daily derived TIT- composites. Special emphasis is given to the effect of an applied coverage correction (CC). Dotted lines show linear trend estimations for IP$_{CC}$. Colored bars are additionally given for a seasonal comparison between November-December (yellowish) and January-March (blueish).

P. 5775 L 10 *"…the here presented last 12 winter-seasons show a positive trend of 20.2 km3."*
Remove decadeˆ(-1). Add "during the analyzed period". See my earlier comment.
We fixed that, thank you for your suggestion.

Thin-ice dynamics and ice production in the Storfjorden polynya for winter-seasons 2002/2003–2013/2014 using MODIS thermal infrared imagery

A. Preußer, S. Willmes, G. Heinemann, and S. Paul

Dept. of Environmental Meteorology, Fac. of Regional and Environmental Sciences, University of Trier, Trier, Germany

Correspondence to: A. Preußer (preusser@uni-trier.de)

Abstract

Spatial and temporal characteristics of the Storfjorden polynya, which forms regularly in the proximity of the islands Spitsbergen, Barentsøya and Edgeøya in the Svalbard archipelago under the influence of strong north-easterly winds, have been investigated for the period 2002/2003 to 2013/2014 using thermal infrared satellite imagery. Thin-ice thicknesses were calculated from MODIS ice-surface temperatures, combined with ECMWF ERA-Interim atmospheric reanalysis data in an energy-balance model. Based on calculated thin-ice thicknesses, associated quantities like polynya area and total ice production were derived and compared to previous remote sensing and modeling studies. A basic coverage-correction scheme was applied to account for cloud-gaps in the daily composites. The sea ice in the Storfjorden area experiences a late fall freeze-up in several years over the 12 winter-period, which becomes most apparent through an increasing frequency of large polynya events until the end of December. During the regarded period, the mean polynya area is $4555.7 \pm 1542.9\,\mathrm{km}^2$. The average ice production in the fjord is estimated with $28.3 \pm 8.5\,\mathrm{km}^3$ per winter and therefore lower than in previous studies. Despite this comparatively short record of 12 winter-seasons, a significant positive trend of $20.2\,\mathrm{km}^3$ per decade could be detected, which contrasts earlier reports of a slightly negative trend in accumulated ice production prior to 2002. Derived estimates underline the importance of this relatively small coastal polynya system considering its contribution to the cold halocline layer through salt release during ice formation processes.

1 Introduction

Recurrent polynyas are considered to play an important role for sea ice production and ocean circulation (Barber and Massom, 2007). The knowledge of ice production in the Arctic is of vital interest for the understanding of the Arctic climate system and the verification of climate and ocean models. Divergent ice motions due to wind are the main cause for the opening of near-coastal polynyas (Smith et al., 1990). During winter, these areas of open

water or thin ice, exposed to the cold atmosphere, are characterized by strong ice production and brine release and modify the atmospheric boundary layer (Ebner et al., 2011; Bauer et al., 2013). The timing, duration and size of a polynya can often have large inter-
30 annual variations because of the general interannual variability of atmosphere-ice-ocean interaction processes (Morales-Maqueda et al., 2004). A precise derivation of the thin-ice thickness (TIT) distribution, the areal extent of a polynya (here defined as open water and thin-ice below 0.2 m) and the amount of local sea ice production is therefore an important step towards a comprehensive understanding of physical processes in the Arctic shelf re-
35 gions and the Arctic sea ice cover in general. Ice production in thin-ice regions can either be estimated by the use of remote sensing methods (Willmes et al., 2010), or by using model approaches (Ebner et al., 2011; Krumpen et al., 2011; Bauer et al., 2013). The use of thermal infrared and microwave remote sensing data offers the opportunity for daily monitoring of thin-ice thicknesses and their distribution on large spatial scales (Yu and Rothrock, 1996;
40 Willmes et al., 2010; Adams et al., 2013).

Storfjorden (see Fig. 1), situated in the southeastern part of the Svalbard archipelago between the main island of Spitsbergen in the west and Barentsøya/Edgeøya in the east, is a region of high coastal polynya activity during winter, as reported by a number of earlier studies (e.g. Haarpaintner et al., 2001; Skogseth et al., 2004). Two shallow straits, Heley-
45 sundet and Freemansundet, connect the northern part of Storfjorden with the Barents Sea and show tidally induced currents as well as exchange processes between water masses inside the fjord and the Barents Sea (Skogseth et al., 2013).

Persistent and strong northerly to north-easterly winds are the main cause for larger polynya openings inside Storfjorden. These opening events may result in large volumes of
50 brine-enriched shelf water, which can be significant regarding the total amount of bottom water in the Arctic Ocean by supplying between 5-20 % of all the newly formed dense water (Skogseth et al., 2004; Hendricks et al., 2011). Besides thermodynamically induced ice growth in Storfjorden during wintertime, the dynamical part due to rafting and deformation processes may play a substantial role in the overall ice thickness distribution, as southerly
55 (onshore) winds can potentially advect sea ice from the Barents Sea into the fjord (Hen-

dricks et al., 2011). An estimation of thermodynamic ice production (IP) within the open water and thin-ice area (i.e. Storfjorden polynya) has been conducted in previous studies using mainly microwave remote sensing (both passive and active systems) in combination with different model approaches. Therein, values are ranging between 20 and 35–45 km^3 for sin-
[60] gle winter-seasons (November–May) between 1997/1998–2000/2001 (Haarpaintner et al., 2001; Skogseth et al., 2004, 2005) and 47 km^3 when averaged over the winter-seasons (October/November–June/July) from 2002/2003–2011/2012 (Jardon et al., 2014). Iwamoto et al. (2014) state that the Storfjorden polynya contributes with around 4 % to the average total ice volume produced in Arctic polynyas between 2002/2003 and 2010/2011 (Septem-
[65] ber to May).

While these estimates make the Storfjorden-area appear to be of minor importance regarding overall ice production in Arctic polynyas, we chose this region due to several distinct requirements. These included the availability of a number of related polynya studies in order to set our estimates into a proper context as well as the comparatively small spatial extent
[70] of the Storfjorden polynya to profit from the enhanced resolution imagery.

Based on daily empirically derived ice thickness distributions in thin-ice areas at a comparatively high spatial resolution, we perform a broad investigation on the associated quantities polynya area and ice-production for the period between 2002/2003 and 2013/2014 using high-resolution Moderate Resolution Imaging Spectroradiometer (MODIS) thermal
[75] infrared data. The presented results will aid to get a more comprehensive understanding of the polynya dynamics in Storfjorden as well as associated processes over both annual and interannual timescales (in the course of this paper, the term "annual" refers to one winter-season from November–March). Further, results will contribute to pan-arctic studies of polynya dynamics.

4

2 Data and methods

2.1 MODIS ice-surface temperatures

Thin-ice thicknesses are computed using the MOD/MYD29 sea-ice product (Hall et al., 2004; Riggs et al., 2006), derived from MODIS satellite data. We used data from both MODIS instruments onboard Terra and Aqua polar-orbiting satellite platforms. It is available from the National Snow and Ice Data Center (NSIDC) located in Boulder, USA (ftp://n5eil01u.ecs.nsidc.org/SAN/). The product contains swath data of ice-surface temperatures (IST). Swath-based IST have a spatial resolution of $1\,km \times 1\,km$ at nadir. The accuracy of the MOD/MYD29 IST is given with 1-3 K (Hall et al., 2004).

For our analysis, swaths covering the Storfjorden area were extracted using meta-data information for each MODIS swath, resulting in 27 individual swaths per day on average for later composite generation. These composites solely consist of nighttime scenes to exclude the influence of incident shortwave radiation (Yu and Lindsay (2003); Adams et al. (2013); compare Ch. 2.3 and 2.3.1). The total number of incorporated MODIS swaths is illustrated in Table 1. As MODIS swath data presumably suffer from inherent panoramic distortion effects, all IST-swaths were mapped onto a $2\,km \times 2\,km$ ($0.018°$) equirectangular grid covering the southern part of Svalbard (75–80° N, 10–30° E).

A polynya mask (red area in Fig. 1) is applied in order to cover an area comparable to previous studies (Skogseth et al., 2004, 2005; Jardon et al., 2014), as well as to limit the probability of remaining hidden cloud artifacts. The mask comprises a total area of $12\,594\,km^2$ and has its southern limit at 77° N (following Skogseth et al., 2004), where a 120 m deep sill serves as kind of a boundary for the accumulation of brine-enriched shelf water in the Storfjorden basin (see Fig. 1).

2.2 ERA-interim reanalysis

For the calculation of TIT, atmospheric variables from the ERA-Interim reanalysis product (Dee et al., 2011) are used to provide 2 m temperature, 2 m dew point temperature, 10 m

5

wind speed components (u and v) and the mean sea-level pressure at a resolution of 6 h. The data set is provided by the European Center for Medium-Range Weather Forecasts (ECMWF) in a horizontal resolution of $0.75°$ (~ 79 km). As the satellite data set is by far spatially higher resolved than the atmospheric data set, a linear interpolation of the ERA-Interim data is performed to match the MODIS data. In the course of the TIT-calculations, each MODIS swath is linked to the closest time step of the atmospheric fields.

2.3 Thin-ice thickness retrieval using a 1-D thermodynamic surface energy model

In order to derive daily TIT-distributions, we use an approach that follows the work of Yu and Rothrock (1996), Yu and Lindsay (2003) and Drucker et al. (2003), with most recent improvements and modifications made by Willmes et al. (2010, 2011) and Adams et al. (2013). The applied method utilizes the distinct relationship between ice surface temperature and thickness of thin ice depending on atmospheric energy fluxes. The IST of very thin ice (with no snow cover) is close to the freezing point of the upper ocean layer and decreasing IST can be observed for thicker ice (Drucker et al., 2003; Kwok et al., 2007). However, IST is governed by atmospheric radiation fluxes and turbulent fluxes of heat, which does not allow for a simple relationship between IST and ice thickness. The thin-ice thickness h_{ice} is therefore calculated using a 1-D thermodynamic sea ice model.

Several assumptions have to be made to apply this model. First, the temperature profile through the ice is assumed to be linear. This approximation is valid for $h_{ice} \leq 0.5$ m (Drucker et al., 2003). Second, the water temperature at the boundary between ice and ocean is constant and at its freezing point ($T_f = 271.35$ K). Third, the ice is assumed to be free of snow. The ice thickness is calculated by using MODIS IST and ERA-Interim reanalysis data. The method is based on the condition, that the conductive heat flux through the ice (Q_{ice}, Eq. 1) equals the total heat flux to the atmosphere (Q_{atm}, Eq. 2). This implies, that all energy

loss at the ice-surface is compensated by the conductive heat flux Q_{ice}.

$$Q_{ice} = \kappa_{ice} \cdot \frac{(T_{surf} - T_f)}{h_{ice}} \tag{1}$$

$$Q_{atm} = Q_0 - H_0 - E_0 \tag{2}$$

135 where Q_0 is the net radiation balance, H_0 and E_0 are the turbulent fluxes of sensible heat and latent heat, respectively, κ_{ice} is the thermal conductivity of sea ice, T_{surf} is the surface temperature, T_f the freezing point of sea water and h_{ice} is the ice thickness. Because of difficulties with the parametrization of shortwave radiation terms (Adams et al., 2013), only nighttime scenes were incorporated into the calculations (by checking the solar incidence
140 angle on a pixel-by pixel basis), so that the radiation balance Q_0 simplifies to the long wave radiation terms $L\downarrow$ and $L\uparrow$. Upwelling longwave radiation $L\uparrow$ is calculated using the IST from MOD/MYD29 with the surface emissivity ϵ_s set to 1. $L\downarrow$ can be obtained using ERA-Interim 2 m temperatures and the atmospheric emissivity ϵ_{atm}, calculated using the formulation of Jin et al. (2006). Turbulent fluxes of sensible (H_0) and latent (E_0) heat in
145 Eq. (2) are calculated using an iterative bulk approach by Launiainen and Vihma (1990), where near surface stratification is considered using Monin–Obukhov similarity theory and associated universal functions for the heat transfer coefficients C_H and C_E. The 10 m wind speed is interpolated to the 2 m level. A constant roughness length for momentum $z_0 = 1 \times 10^{-3}$ m is used. As could be shown by Adams et al. (2013), the standard approach used
150 in previous studies using constant heat transfer coefficients tends to underestimate the ice thickness by approximately 7 cm on average, when compared to an iteratively calculated heat transfer coefficient. To obtain the ice thickness h_{ice}, the total atmospheric flux Q_{atm} (Eq. 2) is set equal to the conductive heat flux through the ice (Q_{ice}; Eq. 1) and Eq. (1) is solved for the ice thickness h_{ice}.

155   TIT is calculated using a value for the thermal conductivity of $\kappa_{ice} = 2.03\,\mathrm{Wm^{-2}\,K^{-1}}$ (Drucker et al., 2003). It is assumed to be uniform at a given pixel location and therefore hypothetical (Tamura and Ohshima, 2011). The described method is only applicable to clear sky conditions, as clouds and fog strongly influence the accuracy of the recorded

7

IST (Riggs et al., 2006). We constrain our analysis to TIT-values ≤ 0.2 m, as this range is
regarded sufficient to get reliable results for ice production (Yu and Rothrock, 1996; Adams et al., 2013).

In a sensitivity analysis of the above described method, Adams et al. (2013) state an uncertainty for the TIT retrieval of ±1.0, ±2.1 and ±5.3 cm for TIT classes 0–5, 5–10 and 10–20 cm, respectively.

2.3.1 Calculation of daily TIT-composites

From all available MODIS swaths covering the Storfjorden polynya region, daily composites of IST and TIT were computed. The TIT is first calculated from each swath on its own with the procedure described in Sect. 2.3. Subsequently, the mean TIT is computed pixel-wise and stored with its corresponding IST value.

By using daily composites, the daily IST-coverage (percentage of pixels within the polynya mask that feature at least one valid IST-value, based on all MOD/MYD29 swaths covering the Storfjorden region at a given day) is significantly increased compared to single swaths, reaching an average value of 82 % for the winter-seasons 2002/2003 to 2013/2014. Figure 2 shows the seasonal and interannual variability of IST-coverage. Noteworthy is a very low coverage in November to early January 2009/2010, as well as generally less frequent coverage at the beginning (November) and end (March) of each winter-season. The latter effect originates from the previously stated restriction to nighttime scenes and consequently a reduction in the amount of available MODIS swaths. Hence, it is also the main reason why the months of October and April were left out in our investigations.

2.3.2 Derivation of ice production and polynya area

Following Tamura et al. (2007, 2008) and Willmes et al. (2011), daily ice production rates are calculated from the heat loss at the ice surface by assuming that the entire heat loss to

8

the overlying atmosphere contributes to new ice formation.

$$\frac{\partial h}{\partial t} = \frac{-\bar{Q}_{\text{ice}}}{\rho_{\text{ice}} \cdot L_{\text{f}}} \tag{3}$$

Therein, $\frac{\partial h}{\partial t}$ stands for the ice production rate, $\bar{Q}_{\text{ice}}$ is the daily mean conductive heat flux through the ice, ρ_{ice} is the density of sea ice (taken as $\rho_{\text{ice}} = 910 \, \text{kg m}^{-3}$) and L_{f} is the latent heat of fusion of ice ($L_{\text{f}} = 0.334 \, \text{MJ kg}^{-1}$; e.g. Tamura and Ohshima, 2011). Note that the negative sign in the right side of Eq. (3) handles the convention that Q_{atm} is con-
190 sidered positive when the surface gains energy, as well as considering that ice production only takes place when there is a net energy loss from the surface. Multiplying $\frac{\partial h}{\partial t}$ with the areal extent of each pixel in the regarded region yields the volume ice production rate $\frac{\partial V}{\partial t}$ (IP). Ice production rates are calculated for each pixel with a TIT $\leq 0.2 \, \text{m}$, and afterwards extrapolated to daily rates for later accumulation and/or averaging. Considering the total
195 polynya area (POLA), a threshold of $h_{\text{ice}} \leq 0.2 \, \text{m}$ is applied to identify TIT-pixels from the daily composites as part of the POLA. The total area of those pixels is then accumulated to obtain the total daily POLA in km^2.

2.3.3 IST-coverage correction

Cloud-induced gaps in our daily TIT and IST composites are a serious problem when we
200 want to compare our initially calculated POLA and IP to estimates from other studies, in which the use of active and passive microwave remote sensing systems largely reduces the effect of atmospheric disturbances.

To overcome these difficulties, a simple scaling approach is applied that works under the assumption, that pixels in the uncovered part of the masked (Fig. 1) daily composites also
205 contribute to the total POLA by approximately the same proportion as those areas that are covered by a IST-signal.

9

The initially calculated daily POLA is therefore scaled by a factor *F*:

$$F = 1/\text{coverage} \tag{4}$$

$$\text{POLA}_{CC} = \text{POLA} \cdot F. \tag{5}$$

The coverage in Eq. (4) could range from 0–1, but we apply the correction only for coverages exceeding 0.5. Similarly, estimated ice production (IP) values are also scaled by the same factor yielding a corrected ice production IP_{CC}.

Application of this correction scheme is limited to cases where the daily IST-coverage (compare Fig. 2) within the fjord (i.e. the predefined polynya mask) surpasses a threshold of 50 %. By using this threshold, unrealistically high POLA_{CC} and IP_{CC} values are avoided. Otherwise, both POLA_{CC} and IP_{CC} are linearly interpolated using bounding days with a coverage fulfilling this precondition.

An error-analysis using clear-sky case-studies revealed that the standard error of the used coverage correction with regards to the POLA parameter amounts to 5-6 %. More information on the performance of this correction scheme can be found in Appendix A.

3 Results

The bars in Fig. 3 show the mean relative contribution of each ice-thickness class from the total number of pixels with a TIT-value ≤ 0.2 m between the winter-seasons 2002/2003 to 2013/2014. A temporal differentiation between the beginning of the freezing season (November–December) and the end of the freezing season (January–March) as well as a combined distribution for the whole winter period is given. Error-bars refer to ± 1 SD of the interannual averaged distribution frequencies. Between November and March, ice thinner than 0.02 m contributes around 15 % to the total polynya area in an average winter-season. Due to a higher sensitivity of open water and very thin ice for sea smoke effects and consequently an exclusion of thin-ice pixels by the cloud mask, this thickness class is potentially biased (Willmes et al., 2011). The average ice thickness within the polynya mask is 10 ± 1.8

10

cm. Thicker ice classes ($> 0.1\,\mathrm{m}$) cover around half of the entire Storfjorden polynya in January to March and show overall lower contributions at the beginning of the freezing season.

This follows from the high contribution of very thin ice in November to December, where over 60 % of the total POLA consists of ice thinner than 0.1 m. SD is highest in the lowest thickness classes ($< 0.04\,\mathrm{m}$) and appear to be lower towards the end of the freezing season, possibly indicating a stronger seasonal variability of ice thickness distributions within the polynya in November and December over the twelve year record (also apparent in relative TIT-frequencies for November–December; Fig. 4).

Spatial distributions of the relative TIT-frequency for 2002/2003 to 2013/2014 are presented as a seasonal comparison between the beginning of each freezing season (November–December, Fig. 4) and the end of each freezing season (January–March, Fig. 5). Therein, a pixel-value of e.g. 0.25 means that on 25 % of all days, a TIT-threshold of 0.2 m was not exceeded. Following the previously stated definition of a polynya, these pixels represent the number of polynya-occurrences in the given period. Figure 5 shows, that the main regions for polynya development towards the end of the freezing season are at the lee-sides of Barentsøya and Edgeøya at the eastern side of the fjord, extending more (2006–2008, 2010, 2012–2014) or less (2003–2005, 2009, 2011) further south-westwards.

At the beginning of the freezing season (Fig. 4), annual distributions show a more variable pattern of TIT-frequencies. In some years (e.g. 2007, 2009, 2012), frequencies exceeding 0.3 cover large areas within the masked area in Storfjorden, which might be an effect of a late fall freeze-up and subsequently longer periods with thin ice and open water in the fjord. In other years (e.g. 2003, 2004), the observed pattern of high TIT-frequencies is similar to typical polynya locations between January and March, indicating an earlier freeze-up of the ice cover in Storfjorden.

Frequent TIT-occurrences in the southern part of Storfjorden could originate from a generally northwards retreating ice edge in Storfjorden in some of the regarded winter-seasons. This becomes most obvious in 2006, 2008 and 2012 to 2014 (Fig. 5). Low values (< 0.05) at the (north-) western side of Storfjorden towards the end of a freezing season (Fig. 5)

further indicate typical fast-ice areas, which are most pronounced in the years 2003, 2004, 2005, 2007, 2009 and 2011.

The daily POLA$_{CC}$ for all winters (November–March) between 2002/2003 and 2013/2014 is presented in Fig. 6. Highest POLA$_{CC}$ values are generally found in November and De-
265 cember, which might be an effect of the already mentioned late fall freeze-up and therefore very thin newly formed ice (compare Figs. 3a and 4) in large parts of Storfjorden. From 2006 to 2008 and 2012 to 2013, this effect even extends well into January with a series of large POLA$_{CC}$ events ($> 5000 \, \text{km}^2$) developing in February and March.

The mean (November to March) POLA for the entire regarded period amounts to $3511.8 \pm$
270 $999.6 \, \text{km}^2$, with an increase of 29 % for POLA$_{CC}$ when the presented coverage correction is applied. Around 60 % of this area consists of ice thinner than 10 cm. A complete overview on wintertime mean POLA and POLA$_{CC}$ values is given in Table 2.

A spatial overview of the resulting accumulated daily ice production rates (in m winter^{-1}), averaged between 2002/2003 and 2013/2014 is presented in Fig. 7. Largest IP occurs in
275 regions which also show high TIT-frequencies (Fig. 5). Average IP values in the western part of Storfjorden are generally lower, as thin-ice in these areas is mainly present at the beginning of the freezing season.

Maximum daily ice production rates in the fjord can reach as high as $26 \, \text{cm d}^{-1}$ (winter-season 2006/2007), with the highest rates occurring on average in the northern part of
280 Storfjorden (north of $77.5° \, \text{N}$).

Figure 8 shows values of accumulated ice production per winter-season from Novem-ber to March, both with and without applied coverage-correction. A detailed overview for each winter-season is additionally given in Table 2. On average, the correction scheme increases the wintertime ice production by approximately 30 %. While average IP-values
285 range between $21.7 \pm 5.9 \, \text{km}^3$ (no CC) and $28.3 \pm 8.5 \, \text{km}^3$ (CC), a high interannual vari-ability of ice production is found, with values as low as $16.1 \, \text{km}^3$ (CC; no CC -16 %) in 2002/2003 and up to $47.2 \, \text{km}^3$ (CC; no CC -31 %) in 2012/2013. Large increases in IP occur from winter 2003/2004 to 2004/2005 (CC: $+7.0 \, \text{km}^3$) and again from winter 2011/2012 to 2012/2013 (CC: $+17.6 \, \text{km}^3$). This could originate from the increasing extent

290 of thin-ice areas in January–March 2005 and 2013 compared to the same period in 2004 and 2012 (Fig. 5). Regardless of an applied coverage correction, a significant ($p \leq 0.05$) positive trend of 1.2–2.0 km^3 yr^{-1} over the examined 12-winter period can be observed. It shows that this trend in overall (Nov.-Mar.) IP$_{CC}$ originates primarily from a significant positive trend (CC: 1.29 km^3 yr^{-1}, $p = 9.05 * 10^{-4}$) at the beginning of winter (November-

295 December), while the period from January-March shows no significant trend (still positive; CC: 0.73 km^3 yr^{-1}, $p = 0.052$). This could be an effect of an observable shift towards more thin-ice in November-December, which is most probably connected to the later appearing fall freeze-up and consequently a lot of open water and very thin ice in the southern part of the applied polynya-mask.

300 **4 Discussion**

In Skogseth et al. (2004, 2005), a manual classification of several ERS-2 synthetic aperture radar (SAR) images from 1998–2002 was performed to derive parameters for a wind-driven polynya width model (Haarpaintner et al., 2001), which gives estimates of ice production and brine-enriched shelf water based on satellite imagery, wind data from nearby weather

305 stations and surface hydrography. Ice production was calculated from surface heat balance and includes contributions from open water (frazil ice), thin ice as well as fast and pack ice inside the Storfjorden basin north of 77° N. This setup was later extended to a 33 year record of modeled total ice production covering the winters 1970 to 2002 using model parameters derived from the examined 5-winter period (Skogseth et al., 2005). While the average total

310 ice production for 1998 to 2002 was estimated to 43.6 ± 9.7 km^3, it was slightly lower for the 33 year time series with only 39.9 ± 11.7 km^3. When comparing these numbers to our average estimate of 28.3 ± 8.5 km^3 (CC) for 2002/2003 to 2013/2014, one has to keep in mind that Skogseth et al. (2004, 2005) also include ice production under fast- and pack-ice inside the fjord, while our study concentrates on open water and thin-ice areas only. Assum-

315 ing an average contribution of 25 % from fast-ice and pack-ice areas (Table 3 in Skogseth et al., 2005) and after reducing annually accumulated total ice production accordingly, the

13

average IP (1970 to 2002) inside open water and thin-ice areas of Skogseth et al. (2005) is lowered to approximately $30 \pm 9\,\text{km}^3$ which is within the here presented SD. Skogseth et al. (2005) give some further information on the interannual variability of ice production within

320 the Storfjorden polynya, although it is stated that the uncertainty for the 33 year time series is increased. The presented 33 year time series shows a slightly negative and non-significant trend of approximately $-2\,\text{km}^3\,\text{decade}^{-1}$, while the here presented last 12 winter-seasons show a positive trend of $2.02\,\text{km}^3\,\text{yr}^{-1}$ during the analyzed period. However, the long-term model-estimates by Skogseth et al. (2005) indicate the presence of multi-decadal fluctua-

325 tions.

Jardon et al. (2014) developed an ice production model which uses Advanced Microwave Scanning Radiometer – EOS (AMSR-E) sea ice concentration data to derive daily open water fractions. Heat flux calculations over water were performed using ERA interim re-analysis data in a bulk algorithm. In contrast to our results, their estimates of POLA and IP

330 incorporate both frazil ice growth as well as ice growth under ice thicker than 20 cm. In comparison, our results should profit from the enhanced resolution of MODIS and daily derived TIT-distributions. Nevertheless, derived POLA from TIT $\leq 0.2\,\text{m}$ in our study compares well with POLA derived from AMSR-E sea ice concentration data. Both wintertime mean POLA and POLA$_{\text{CC}}$ are within the 25th and 75th percentile of the estimated open water area by

335 Jardon et al. (2014) in almost every winter-season, except for 2004/2005 and 2010/2011, where both values derived by MODIS exceed the 75th percentile. Discrepancies in derived total ice production are obvious, but can be partly explained by differences in the regarded time frame of each winter-season. While Jardon et al. (2014) analyze the full period with sea ice in the fjord (roughly October/November to June/July), we focus on the November

340 to March period. Even if we reduce the presented IP-values by the amount of frazil ice that is formed in the months April–July, which in 2006/2007 (exemplary shown in Jardon et al., 2014) contributed with around 15 % to the total volume of frazil ice in this particular winter-season, the time series are differing on average by approx. 40 %. Thereby, Jardon et al. (2014) presents higher IP-values in all winter-seasons except 2004/2005 and 2010/2011,

345 but overall the interannual variability is comparable.

14

The studies by Tamura and Ohshima (2011) and Iwamoto et al. (2014) are facing similar restrictions concerning the spatial resolution of the applied passive microwave data from Special Sensor Microwave Imager (SSM/I) and AMSR-E, which is most apparent in smaller polynyas such as in Storfjorden. In Tamura and Ohshima (2011), an average ice production of $137\pm35\,\mathrm{km^3}$ for the period 1992–2007 (September–May) is presented. This value largely exceeds our estimates as well as those by Skogseth et al. (2005) and Jardon et al. (2014), most probably due to the discrepancies in spatial resolution of the input data. More recent numbers by Iwamoto et al. (2014), who use an updated algorithm based on MODIS TIT, AMSR-E and ERA-Interim reanalysis, are also lower than those in Tamura and Ohshima (2011), with the mean annual (also September–May) ice production between 2002/2003 and 2010/2011 being estimated as $47\pm5\,\mathrm{km^3}$ (roughly $40\,\mathrm{km^3}$ for November–March; based on presented monthly mean values). A positive trend of $3\,\mathrm{km^3}$ per decade is presented, which is much smaller than our value of $18.7\,\mathrm{km^3}$ per decade based on the same period from 2002/2003 to 2010/2011. Although Iwamoto et al. (2014) provide enhancements in terms of spatial resolution and the inclusion of land-fast ice detection in comparison to Tamura and Ohshima (2011), our estimates are still exceeded in every winter-season. The presented interannual variability is similar to our study, with 2005/2006 and 2008/2009 being the only winter-seasons with a strongly contrasting development. Both Tamura and Ohshima (2011) and Iwamoto et al. (2014) apply noticeably larger polynya masks to derive ice production values in the Storfjorden area, which extend well into the Greenland and Barents Sea regions and far beyond Storfjorden itself. This omission of local characteristics in the Storfjorden basin in addition to a differing base period, which spans the months from September to May, could therefore explain part of the difference. However, the use of coarse resolution passive microwave data certainly leads to a higher uncertainty of IP-estimates, while the sign of the bias cannot be determined here. It will depend on the distribution of thin ice within the sensor's footprint and potential land spillover effects.

5 Summary and conclusions

In this study, we presented a comprehensive overview of daily thin-ice thickness distributions and resulting thermodynamic ice-production rates for the Storfjorden polynya, located
in the southern part of the Svalbard archipelago. The investigation period covers the winter-seasons 2002/2003–2013/2014 from November to March. Our results are complementary to previous studies in the Storfjorden region (e.g. Skogseth et al., 2004, 2005; Hendricks et al., 2011) and underline the importance of this polynya considering the total amount of ice production and accompanied salt release each winter-season, despite its comparatively small spatial extent. Within the polynya, ice thicknesses below 10 cm are dominating in the course of an average winter-season and cover larger areas in the eastern part of Storfjorden. This enables ice-production rates, which sum up to an average value of $28.3 \pm 8.5\,\mathrm{km^3}$ per winter-season. There is a positive trend in accumulated ice production over the last 12 winter-seasons which contrasts earlier indications of a slightly negative trend prior to 2002 (Skogseth et al., 2005).

Compared to other studies which rely on active and passive microwave remote sensing, the use of MODIS IST has distinct drawbacks considering the effect of clouds, which produce data gaps if correctly identified by the MODIS cloud mask and possibly erroneous IST-values if nighttime clouds remain undetected. By composing daily composites, data gaps in the Storfjorden region were minimized resulting in an average IST-coverage of 82 % within the applied polynya mask. The application of a coverage-correction scheme yielded plausible adjustments of approximately 30 % to the total polynya area and ice production, although its current basic approach offers room for future improvements like e.g. including long-term spatial statistics. Still, this comprehensive data set will be of high value for a variety of climate and ocean applications, including the provision of quasi-daily high-resolution thin-ice thickness charts for regional climate and ocean models.

Appendix A: Uncertainty of the applied IST-coverage correction

We selected a total of six case studies from January 2009 (DOY 002, 020, 024, 025, 026, 030), which feature near clear-sky conditions (IST-coverage $\geq$ 99%). The coverage-correction has been applied for each case study after randomly removing 45 % of the pixels within the polynya mask for 1000 realizations. The resulting deviation (in %) from the "true" polynya area (POLA) from all case studies combined is shown in Fig. 9. POLA$_{CC}$-deviations almost perfectly follow a typical normal (Gaussian) distribution, with a mean value of 0.67 % and a standard error of 5-6 % of the daily POLA.

Alternatively, we think that interpolating between bounding days with better IST-coverage ($>$ 50%) is so far the best solution of handling large cloud-gaps in the daily composites.

As the correction of IP-values uses the same scaling-factor F, the retrieved error-margins can also be regarded as the uncertainty of our IP$_{CC}$ estimates.

References

Adams, S., Willmes, S., Schroeder, D., Heinemann, G., Bauer, M., and Krumpen, T.: Improvement and sensitivity analysis of thermal thin-ice retrievals, IEEE Transactions on Geoscience and Remote Sensing, 51, 3306–3318, doi:10.1109/tgrs.2012.2219539, 2013.

Barber, D. G. and Massom, R. A.: The Role of Sea Ice in Arctic and Antarctic Polynyas, in: Polynyas - Windows to the World, edited by Smith, W. O. and Barber, D. G., chap. The Role of Sea Ice in Arctic and Antarctic Polynyas, pp. 1–54, Elsevier Oceanography Series, doi:10.1016/s0422-9894(06)74001-6, 2007.

Bauer, M., Schröder, D., Heinemann, G., Willmes, S., and Ebner, L.: Quantifying polynya ice production in the Laptev Sea with the COSMO model, Polar Research, 32,

doi:10.3402/polar.v32i0.20922, http://www.polarresearch.net/index.php/polar/article/view/20922, 2013.

Dee, D. P., Uppala, S. M., Simmons, A. J., Berrisford, P., Poli, P., Kobayashi, S., Andrae, U., Balmaseda, M. A., Balsamo, G., Bauer, P., Bechtold, P., Beljaars, A. C. M., van de Berg, L., Bidlot, J., Bormann, N., Delsol, C., Dragani, R., Fuentes, M., Geer, A. J., Haimberger, L., Healy, S. B., Hersbach, H., Hólm, E. V., Isaksen, L., Kållberg, P., Köhler, M., Matricardi, M., McNally, A. P., Monge-Sanz, B. M., Morcrette, J.-J., Park, B.-K., Peubey, C., de Rosnay, P., Tavolato, C., Thépaut, J.-N., and Vitart, F.: The ERA-Interim reanalysis: configuration and performance of the data assimilation system, Quarterly Journal of the Royal Meteorological Society, 137, 553–597, doi:10.1002/qj.828, 2011.

Drucker, R., Martin, S., and Moritz, R.: Observations of ice thickness and frazil ice in the St. Lawrence Island polynya from satellite imagery, upward looking sonar, and salinity/temperature moorings, J. Geophys. Res., 108, 3149, doi:10.1029/2001jc001213, 2003.

Ebner, L., Schröder, D., and Heinemann, G.: Impact of Laptev Sea flaw polynyas on the atmospheric boundary layer and ice production using idealized mesoscale simulations, Polar Research, 30 (7210), 16, doi:10.3402/polar.v30i0.7210, 2011.

Haarpaintner, J., Gascard, J.-C., and Haugan, P. M.: Ice production and brine formation in Storfjorden, Svalbard, Journal of Geophysical Research: Oceans (1978–2012), 106, 14 001–14 013, doi:10.1029/1999jc000133, http://onlinelibrary.wiley.com/doi/10.1029/1999JC000133/full, 2001.

Hall, D., Key, J., Casey, K., Riggs, G., and Cavalieri, D.: Sea ice surface temperature product from MODIS, Geoscience and Remote Sensing, IEEE Transactions on, 42, 1076 – 1087, doi:10.1109/tgrs.2004.825587, 2004.

Hendricks, S., Gerland, S., Smedsrud, L., Haas, C., Pfaffhuber, A., and Nilsen, F.: Sea-ice thickness variability in Storfjorden, Svalbard, Annals of Glaciology, 52, 61–68, doi:10.3189/172756411795931561, http://www.ingentaconnect.com/content/igsoc/agl/2011/00000052/00000057/art00008, 2011.

Iwamoto, K., Ohshima, K. I., and Tamura, T.: Improved mapping of sea ice production in the Arctic Ocean using AMSR-E thin ice thickness algorithm, Journal of Geophysical Research: Oceans, 119, 3574–3594, doi:10.1002/2013jc009749, http://onlinelibrary.wiley.com/doi/10.1002/2013JC009749/abstract, 2014.

Jakobsson, M., Mayer, L., Coakley, B., Dowdeswell, J. A., Forbes, S., Fridman, B., Hodnesdal, H., Noormets, R., Pedersen, R., Rebesco, M., Schenke, H. W., Zarayskaya, Y., Accettella, D., Armstrong, A., Anderson, R. M., Bienhoff, P., Camerlenghi, A., Church, I., Edwards, M., Gard-

18

ner, J. V., Hall, J. K., Hell, B., Hestvik, O., Kristoffersen, Y., Marcussen, C., Mohammad, R., Mosher, D., Nghiem, S. V., Pedrosa, M. T., Travaglini, P. G., and Weatherall, P.: The international bathymetric chart of the Arctic Ocean (IBCAO) version 3.0, Geophysical Research Letters, 39, doi:10.1029/2012gl052219, 2012.

Jardon, F., Vivier, F., Bouruet-Aubertot, P., Lourenço, A., Cuypers, Y., and Willmes, S.: Ice production in Storfjorden (Svalbard) estimated from a model based on AMSR-E observations: Impact on water mass properties, Journal of Geophysical Research: Oceans, 119, 377–393, doi:10.1002/2013jc009322, http://onlinelibrary.wiley.com/doi/10.1002/2013JC009322/full, 2014.

Jin, X., Barber, D., and Papakyriakou, T.: A new clear-sky downward longwave radiative flux parameterization for Arctic areas based on rawinsonde data, J. Geophys. Res., 111, D24 104, doi:10.1029/2005jd007039, 2006.

Krumpen, T., Hölemann, J. A., Willmes, S., Maqueda, M., Busche, T., Dmitrenko, I. A., Gerdes, R., Haas, C., Heinemann, G., Hendricks, S., et al.: Sea ice production and water mass modification in the eastern Laptev Sea, Journal of Geophysical Research: Oceans (1978–2012), 116, doi:10.1029/2010JC006545, 2011.

Kwok, R., Comiso, J. C., Martin, S., and Drucker, R.: Ross Sea polynyas: Response of ice concentration retrievals to large areas of thin ice, J. Geophys. Res., 112, C12 012, doi:10.1029/2006jc003967, 2007.

Launiainen, J. and Vihma, T.: Derivation of turbulent surface fluxes - An iterative flux-profile method allowing arbitrary observing heights, Environmental Software, 5, 113–124, doi:10.1016/0266-9838(90)90021-w, 1990.

Morales-Maqueda, M., Willmott, A., and Biggs, N.: Polynya dynamics: A review of observations and modeling, Reviews of Geophysics, 42, 1–37, doi:10.1029/2002rg000116, 2004.

Riggs, G., Hall, D., and Salomonson, V.: MODIS Sea Ice Products User Guide to Collection 5, National Snow and Ice Data Center, University of Colorado, Boulder, CO 80309-0449 USA, http://nsidc.org/data/docs/daac/modis_v5/dorothy_ice_doc.pdf, 2006.

Skogseth, R., Haugan, P., and Haarpaintner, J.: Ice and brine production in Storfjorden from four winters of satellite and in situ observations and modeling, Journal of Geophysical Research: Oceans (1978–2012), 109, doi:10.1029/2004jc002384, 2004.

Skogseth, R., Fer, I., and Haugan, P. M.: Dense-Water Production and Overflow from an Arctic Coastal Polynya in Storfjorden, The Nordic Seas: An Integrated Perspective, pp. 73–88, doi:10.1029/158gm07, http://onlinelibrary.wiley.com/doi/10.1029/158GM07/summary, 2005.

19

Skogseth, R., McPhee, M. G., Nilsen, F., and Smedsrud, L. H.: Creation and tidal advection of a cold salinity front in Storfjorden: 1. Polynya dynamics, Journal of Geophysical Research: Oceans, 118, 3278–3291, doi:10.1002/jgrc.20231, http://onlinelibrary.wiley.com/doi/10.1002/jgrc.20231/full, 2013.

Smith, S. D., Muench, R. D., and Pease, C. H.: Polynyas and leads: An overview of physical processes and environment, Journal of Geophysical Research, 95, 9461–9479, doi:10.1029/jc095ic06p09461, 1990.

Tamura, T. and Ohshima, K. I.: Mapping of sea ice production in the Arctic coastal polynyas, J. Geophys. Res., 116, C07 030, doi:10.1029/2010jc006586, 2011.

Tamura, T., Ohshima, K. I., Markus, T., Cavalieri, D. J., Nihashi, S., and Hirasawa, N.: Estimation of Thin Ice Thickness and Detection of Fast Ice from SSM/I Data in the Antarctic Ocean, J. Atmos. Oceanic Technol., 24, 1757–1772, doi:10.1175/jtech2113.1, 2007.

Tamura, T., Ohshima, K. I., and Nihashi, S.: Mapping of sea ice production for Antarctic coastal polynyas, Geophys. Res. Lett., 35, L07 606, doi:10.1029/2007gl032903, 2008.

Willmes, S., Krumpen, T., Adams, S., Rabenstein, L., Haas, C., Hoelemann, J., Hendricks, S., and Heinemann, G.: Cross-validation of polynya monitoring methods from multisensor satellite and airborne data: a case study for the Laptev Sea, Canadian Journal of Remote Sensing, 36, S196–S210, doi:10.5589/m10-012, 2010.

Willmes, S., Adams, S., Schröder, D., and Heinemann, G.: Spatio-temporal variability of polynya dynamics and ice production in the Laptev Sea between the winters of 1979/80 and 2007/08, Polar Research, 30 (5971), 16, doi:10.3402/polar.v30i0.5971, 2011.

Yu, Y. and Lindsay, R.: Comparison of thin ice thickness distributions derived from RADARSAT Geophysical Processor System and advanced very high resolution radiometer data sets, J. Geophys. Res., 108, 3387, doi:10.1029/2002jc001319, 2003.

Yu, Y. and Rothrock, D. A.: Thin ice thickness from satellite thermal imagery, J. Geophys. Res., 101, 25 753–25 766, doi:10.1029/96jc02242, 1996.

Table 1. Total number of individual MODIS swaths, which were incorporated into the TIT-calculations. Numbers are given for each winter-season from November to March.

Winter-season	Number of MODIS swaths
2002–2003	4054
2003–2004	4023
2004–2005	4062
2005–2006	4073
2006–2007	3990
2007–2008	4069
2008–2009	4135
2009–2010	4142
2010–2011	4205
2011–2012	4129
2012–2013	4137
2013–2014	4244
Sum	49 263

Table 2. Accumulated ice production in $km^3\,winter^{-1}$ and average polynya area (in km^2) each winter-season (November to March) in the Storfjorden polynya, together with the interannual average (Mean) and its SD. CC denote values after coverage correction, with relative increase compared to uncorrected values in brackets. All values are calculated within the predefined polynya mask (Fig. 1).

|	Acc. IP (km^3)	Acc. IP$_{CC}$ (km^3)	POLA (km^2)	POLA$_{CC}$ (km^2)
2002–2003	13.9	16.1 ($+16\%$)	2185.2	2429.6 ($+11\%$)
2003–2004	15.2	16.7 ($+10\%$)	2186.6	2382.0 ($+9\%$)
2004–2005	19.2	23.7 ($+24\%$)	2684.7	3296.6 ($+23\%$)
2005–2006	20.6	25.1 ($+22\%$)	3934.8	4750.6 ($+21\%$)
2006–2007	19.4	25.3 ($+31\%$)	3473.9	4524.2 ($+30\%$)
2007–2008	27.4	33.1 ($+21\%$)	4491.0	5472.5 ($+22\%$)
2008–2009	21.6	24.6 ($+14\%$)	2965.4	3353.3 ($+13\%$)
2009–2010	17.3	30.0 ($+73\%$)	3390.1	6357.0 ($+88\%$)
2010–2011	23.2	31.9 ($+38\%$)	2996.0	4024.7 ($+34\%$)
2011–2012	21.5	29.6 ($+38\%$)	4087.6	5001.5 ($+22\%$)
2012–2013	36.0	47.2 ($+31\%$)	5592.4	7388.0 ($+32\%$)
2013–2014	25.4	36.5 ($+44\%$)	4154.3	5688.4 ($+37\%$)
Mean	21.7	28.3 ($+30\%$)	3511.8	4555.7 ($+29\%$)
SD	5.9	8.5	999.6	1542.9
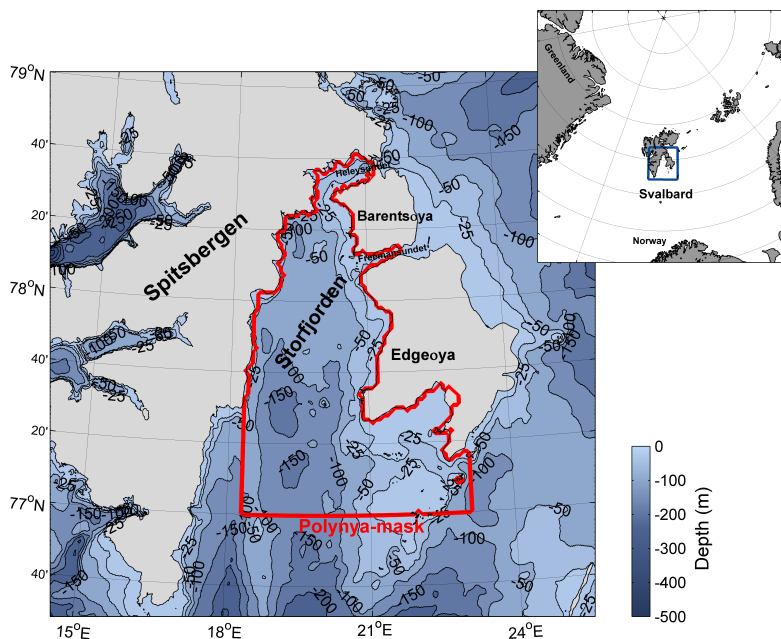
Figure 1. Map of the Svalbard archipelago in western Barents Sea. The study region is located in Storfjorden, which is surrounded by the main island Spitsbergen in the west and Barentsøya/Edgeøya in the east. The applied polynya mask is marked in red, enclosing the Storfjorden basin north of the sill at 77° N. Bathymetric data by Jakobsson et al. (2012) (IBCAO v3.0).
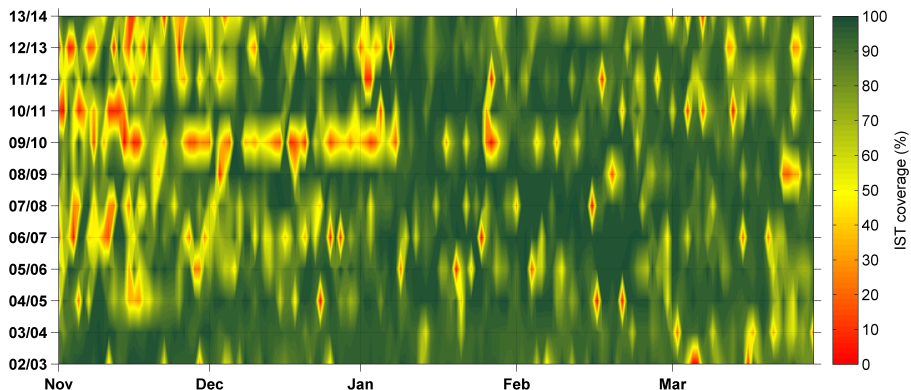
Figure 2. Interannual overview of the daily IST-coverage (%) within the applied polynya mask (compare Fig. 1). Values are derived from daily MODIS IST-composites for the complete investigation period from 2002/2003 to 2013/2014 (November–March).
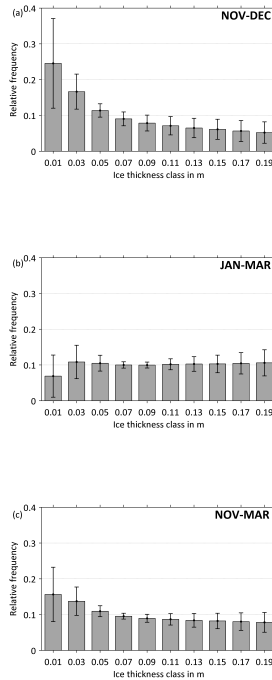
Figure 3. Relative TIT-distribution in the Storfjorden polynya, with ice thickness classes of 2 cm range (x axis). Input data is based on daily TIT-composites. The bars indicate the mean relative distribution of each thickness class from the total number of TIT $\leq$ 0.2 m appearances between the winter-seasons 2002/2003 to 2013/2014. Error bars refer to ± 1 SD. Besides an overview of the complete freezing season from November to March **(c)**, it is further separated between the months November to December **(a)** as well as January to March **(b)**.
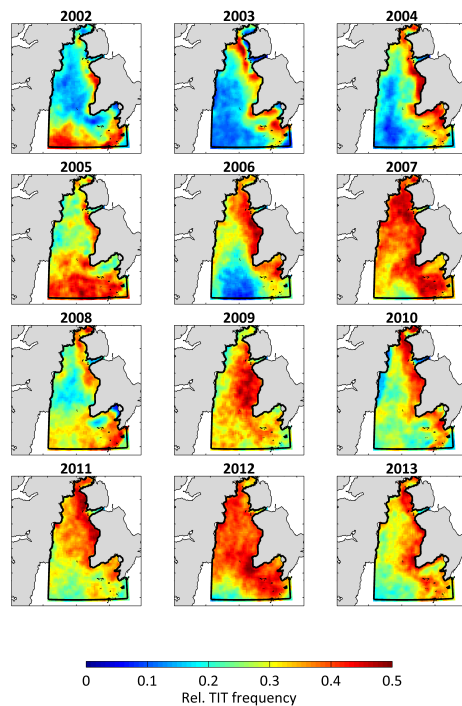
Figure 4. Early freezing season (November to December) relative frequency distribution of TIT ≤ 0.2 m for 2002 to 2013, based on daily TIT-composites.
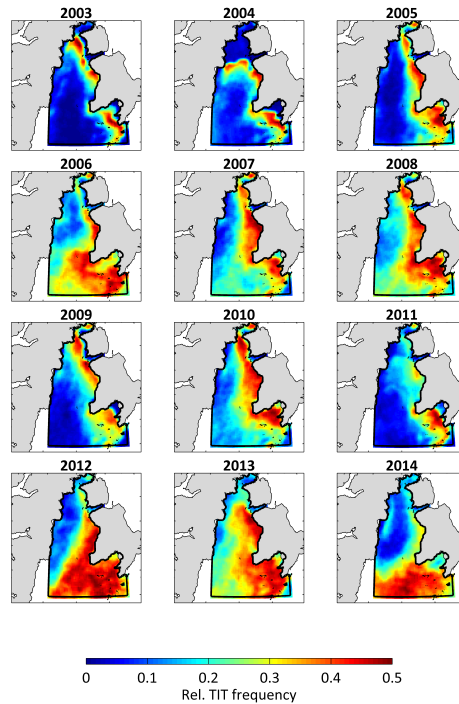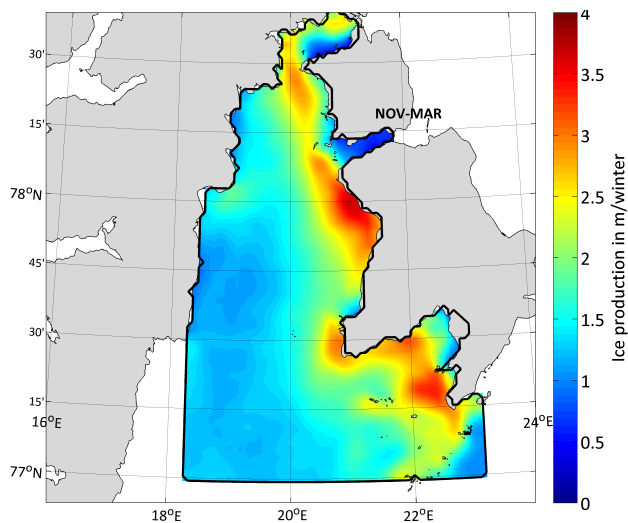
Figure 5. Late freezing season (January to March) relative frequency distribution of TIT ≤ 0.2 m for 2003 to 2014, based on daily TIT-composites.
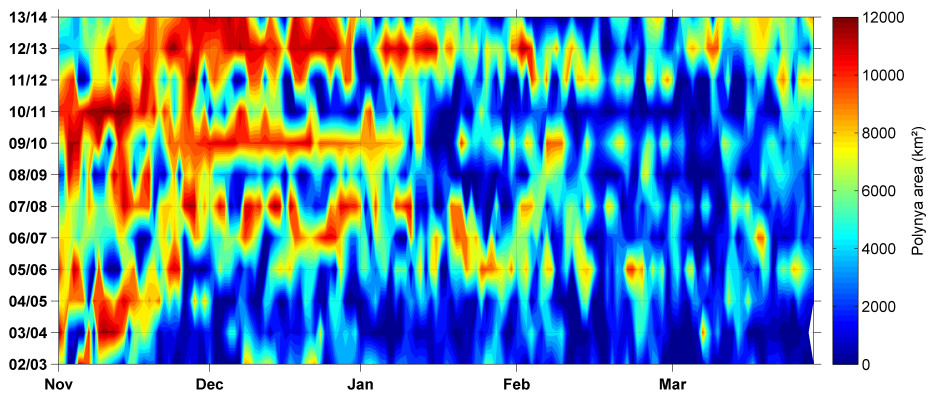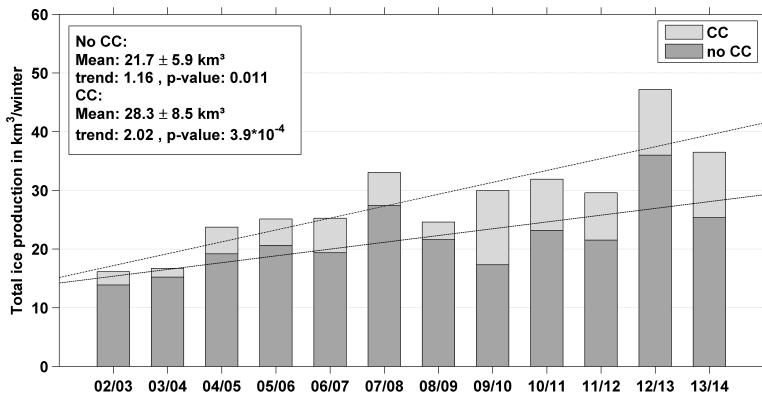
Figure 6. Hovmoeller diagram of daily POLA$_{CC}$ (TIT ≤ 0.2 m) in the Storfjorden polynya between 2002/2003 and 2013/2014.

Figure 7. Spatial distribution of the interannual mean accumulated IP rate in $\mathrm{m\,winter^{-1}}$. Values are first accumulated for each winter-season from November to March and afterwards averaged for 2002/2003 to 2013/2014.

Figure 8. Annual wintertime accumulated ice production in the Storfjorden polynya, given in $km^3\,winter^{-1}$. Estimations are based on daily heat flux calculations using the daily derived TIT-composites. Special emphasis is given to the effect of an applied coverage correction (CC). Dotted lines show linear trend estimations for both IP and IP_{CC}.
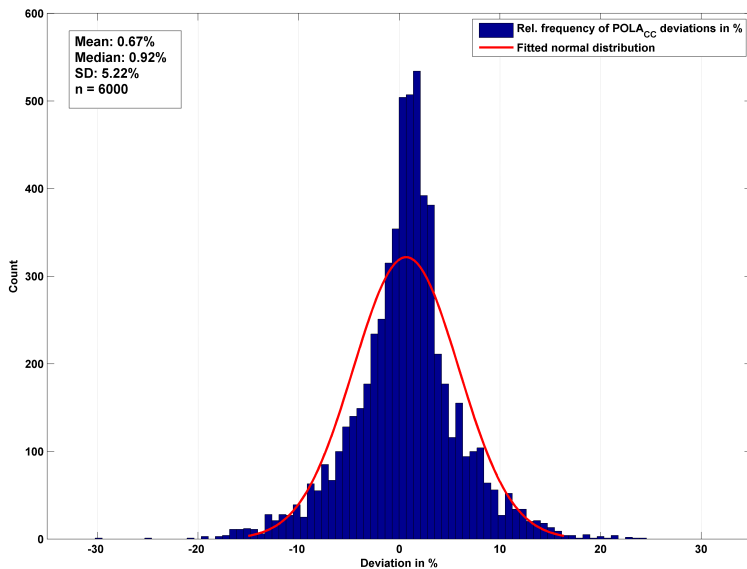
Figure 9. Histogram of POLA$_{CC}$-deviations, based on six near clear-sky case studies from January 2009 (DOY: 002, 020, 024, 025, 026, 030). For each case study, the coverage-correction was repeated several times (n=1000*6), after randomly removing 45% of the pixels within the applied polynya mask.The red curve illustrates a fitted normal distribution.